Modeling of Channel Asymmetry in HAP-based Optical Wireless Communications

Neha Tiwari[a], Swades De[b,a], and S. Dharmaraja[c,a]
[a]Bharti School of Telecommunication, IIT Delhi, New Delhi, India
[b] Department of Electrical Engineering, IIT Delhi, New Delhi, India
[c] Department of Mathematics, IIT Delhi, New Delhi, India

***Abstract*—This paper examines the asymmetry in the optical wireless communication channel from and to high-altitude platform stations (HAPs). The effects of anisotropic and variable-sized eddies in the atmosphere on the bidirectional laser links in terms of fluctuation of beam spot size, position, and intensity are studied. Additionally, it is demonstrated that the spatial impulse responses of the anisotropic channel are different for the forward and reverse paths of the laser beam. Through detailed phase-screen simulations of beam evolution through the turbulent atmosphere in both the downlink and uplink channels, the probability distribution function of channel gains is developed and compared. This study assumes importance in deciding on optimal link budgets, such as forward error correction, adaptive optics, and diversity reception, thereby aiding in increased data rate or link distance in HAP-to-ground optical wireless communications.**

***Index Terms*—Free-space optical communication, channel asymmetry, anisotropic turbulence, HAP-to-ground communication**

I. Introduction

High-altitude platforms (HAPs) offer a promising new communication option that combines the benefits of terrestrial and satellite communication systems for achieving broadband connectivity to users at a low cost. They are simple to deploy and maintain, making them an excellent alternative for network operators looking for ways to expand coverage to meet the rising demand for additional capacity. HAPs are aircraft or airships, generally placed in the stratosphere at a typical height of 17 to 25 km [1]. Integrating HAPs and free space optical (FSO) communications is a promising solution to establishing high data rate aerial links for the next generation wireless networks. However, space limitations, such as the detrimental effects of the earth's turbulent atmosphere on a laser beam's ability to communicate at that altitude, make it challenging to implement HAP-based FSO links. Random fluctuations of temperature and pressure in the earth's atmosphere cause turbulence in the form of eddies. The microscale fluctuations in refractivity lead to elevation-dependent uncertainties. The refractivity fluctuations are extreme near the ground and decrease with height.

On the other hand, eddy size in the atmosphere keeps increasing as we move away from the surface. The shape of the eddies also changes from being spherical and symmetrical near the ground to being highly asymmetrical and anisotropic at heights far away from the ground [2]. Therefore a laser beam propagating to a HAP receiver situated at an altitude of 17 to 25 km in the stratosphere will experience a very different turbulent atmosphere than a beam traveling towards a ground-based optical receiver. These highly dynamic processes in the atmosphere contribute considerably to the error budget of the laser beam links to the HAPs.

A. Background and motivation

Asymmetry in the ground-satellite based, bidirectional laser communication channel has been discussed in the literature [3, 4]. However, the primary distinction between uplink and downlink transmission in ground-satellite laser communication results from the fact that, during uplink, the beam first encounters the atmosphere, where it has a positive curvature and a small beam size. After that, it travels through vacuum space, where it only faces spreading in free space. In contrast, during downlink transmission, the beam first undergoes diffraction effects during free-space propagation in space and then encounters the atmosphere with a large beam size, which possesses essentially no curvature at this point. In bidirectional optical communication link between HAPs and ground station the main effects induced by the atmosphere happen between zero altitude and 20 km. In this paper we show that the uplink and downlink transmissions possess key differences, mainly arising from the interplay between the sizes of the beam and the turbulent eddies.

Furthermore, the Kolmogorov power spectrum model for the refractive index is frequently used in research to simulate atmospheric turbulence, a critical problem for optical wireless FSO channels [3, 5]. However, recent studies have shown that the statistical behavior of the atmosphere is not well captured by the Kolmogorov power spectrum model since there are physical concerns that are not covered by the classical Kolmogorov theory [2]. Studies have shown that optical turbulence only adheres to the Kolmogorov power spectrum model inside the atmospheric boundary layer (1-2 km), with a few deviations occurring extremely close to the ground [6, 7]. Optical turbulence can be anisotropic at large spatial scales in the free atmosphere, especially within the stably layered stratosphere. The Kolmogorov power spectrum may not accurately characterize the actual turbulence behavior. In the upper troposphere and lower stratosphere, Kyrazis et al. [8] measured non-Kolmogorov turbulence and concluded that the velocity and temperature changes might not follow the same law as predicted by Kolmogorov's theory.

In this paper, we have modeled the FSO channel focusing on two main points: anisotropy and power laws, that are different from Kolmogorov law. Studying the impact of the turbulent environment is crucial for simultaneous pre- as well as post-processing of bidirectional laser beams and implementation of techniques like forward error correction, adaptive optics, and diversity reception which help to increase the data throughput or link distance while lowering the bit error ratio and outage risk of the optical HAP communication systems.

B. Paper organization

The rest of the paper is organized as follows. Section II introduces the system model used for analytical and simulation work. The focus of Section III is on the proof of the presence of non-reciprocity in the channel to and from HAPs and discusion of various optical effects on laser beam propagation in forward and reverse directions. Numerical results are discussed in Section IV and conclusions are drawn in Section V.

II. SYSTEM MODEL

The propagation geometry for line-of-sight free space optical communication through the turbulent atmosphere is shown in Fig. 1. The forward-path propagation consists of a transmitter at the optical ground station equipped with a laser system to communicate through a HAP receiver. The reverse-path propagation consists of a HAP transmitter and a ground-based optical receiver. For our analysis, the FSO channel model is split into two layers: the atmospheric boundary layer (up to 2 km in altitude), where heating of the surface causes convective instability, and the free atmosphere (above the atmospheric boundary layer), where the friction caused by the Earth's surface has little impact on air motion. Optical turbulence is assumed to be homogeneous and isotropic inside the atmospheric boundary layer, where the Kolmogorov power spectrum model of the refractive index is typically accurate inside the inertial sub range. Above 2 km, the optical turbulence is assumed to be anisotropic, and the Kolmogorov power spectrum does not accurately capture the genuine turbulence behavior. We have used the anisotropic power spectrum for this region to model the refractive-index fluctuations given in [2].

Near the ground, the inner scale l_0 of turbulent eddies is in the order of millimeters, whereas the outer scale L_0 might have values in meters. Moving vertically away from the earth causes both values to increase. Since altitude impacts the eddies' shape as well [9], we have assumed that the eddies in the atmospheric boundary layer (0–2 km of altitude) are small and rather symmetrical. In contrast, the irregularities in eddy shapes above 2 km are assumed to be ellipsoidal, meaning the eddies flatten out more in the horizontal direction, as depicted in Fig. 1. Within the atmospheric boundary layer the turbulence is modelled as moderate-to- strong turbulence because near ground refractive index fluctuations are large i.e. $C_n^2 \geq 10^{-13}m^{2/3}$ and up to 2 km the value of C_n^2 vary between $10^{-13}m^{2/3}$ to $10^{-16}m^{2/3}$. Above 2 km, the turbulence is modelled as weak because $C_n^2 \leq 10^{-16}m^{2/3}$ [10]. Hence, a laser beam first encounters a very strong turbulence region and then moves towards a weak turbulence region during forward path propagation geometry from an optical ground station to the HAP receiver. During the reverse propagation geometry, the beam from a HAP transmitter will first encounter a weak turbulence region and then strong turbulence near the optical receiver situated at the ground.

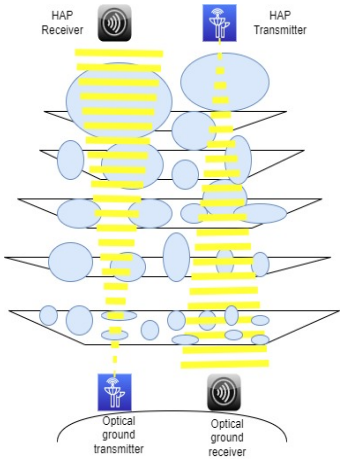

Fig. 1: Schematic model of ground-HAP FSO channel with variable sized eddies.

At the receiver, the optical signal after conversion to baseband signal is expressed as [11]

$$y = \eta_e h s + n, \tag{1}$$

where s stands for on-off keying (OOK) modulated optical signal. The average power in s is given by $\sigma_s^2 = \mathbb{E}\{|s|^2\}$, $h \in \mathbb{R}^+$ is the channel gain, η_e is the effective optical-to-electrical conversion ratio and n is additive white Gaussian noise (AWGN) with zero mean and variance σ_n^2. FSO channels are generally affected by atmospheric losses, geometric and misalignment losses, and atmospheric turbulence. For the sake of simplicity, we assume flawless beam tracking and constant transmitter and receiver positions. As a result, the jitter-related misalignment losses can be disregarded. Then, the channel gain h affecting the Rx irradiance between the laser system and photodetector (PD) can be modeled as

$$h = h_l h_g h_a, \tag{2}$$

where h_l is the atmospheric path loss described by Beer–Lambert's law, which is deterministic and taken to be unity throughout this work without loss of generality. h_a and h_g are random atmospheric turbulence component and geometric losses, respectively. The effects of the atmosphere on a propagating beam are modeled using the multiple phase screen (MPS) model. The transmitter is equipped with a laser source emitting a Gaussian beam which is propagated through turbulence with the initial field distribution given by

$$U(\mathbf{r}) = exp\left[-\frac{2r^2}{d^2} - \frac{ikr^2}{2F}\right]. \tag{3}$$

where, F is the radius of curvature (we have taken collimated beam), d is the beam diameter.

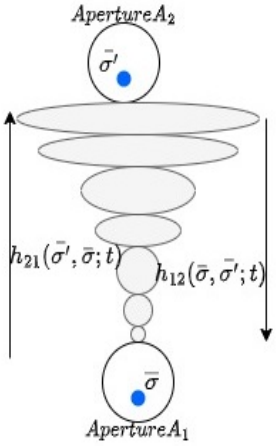

Fig. 2: Channel model geometry.

III. Channel non-reciprocity and its effect on Optical Links

Here, given the Gaussian laser beam in (3), first, we depict the channel non-reciprocity for vertical optical communication links. Next, we study the optical effects of asymmetric FSO channel on the propagation of Gaussian laser beams. Fig. 2 is based on the notion that the turbulence state is stationary. A_1 and A_2 depict two parallel transmitting and receiving antenna apertures separated by a channel filled with variable-sized eddies. A monochromatic scalar-wave theory will do as we will assume that the transmitted beam is linearly polarised. With these assumptions, generality is not lost. The sub-picosecond multipath dispersion caused by turbulence and the millisecond turbulence coherence time are both substantially shorter than the nanosecond-duration pulses used in Gbps transmission [12]. Additionally, it is known that turbulence does not result in depolarization [13].

A. Forward and reverse path propagation

Let $U(\bar{\sigma})$ represents a complex field amplitude transmitted from A_1 and $U(\bar{\sigma'})$ is the field amplitude received at A_2 at time t , then

$$U(\bar{\sigma'}; t) = \int_{A_1} U(\bar{\sigma}) h_{21}(\bar{\sigma'}, \bar{\sigma}; t)\, d\bar{\sigma}. \tag{4}$$

For the reverse path let $U(\bar{\sigma'})$ represent a complex field amplitude transmitted from A_2 and $U(\bar{\sigma})$ is the field amplitude received at A_1 at time t , then

$$U(\bar{\sigma}; t) = \int_{A_2} U(\bar{\sigma'}) h_{12}(\bar{\sigma}, \bar{\sigma'}; t)\, d\bar{\sigma'}. \tag{5}$$

Here, h_{21} and h_{12}, are the impulse responses that characterize propagation between A_1 and A_2. For the free space, these impulse responses satisfy reciprocity condition i.e. $h_{21}(\bar{\sigma'}, \bar{\sigma}) = h_{12}(\bar{\sigma}, \bar{\sigma'})$. The time parameter is ignored as free-space channel is time-invariant. In an anisotropic turbulent channel h_{21} and h_{12} represent field amplitudes due to anisotropic point sources. Shapiro, Jeffrey H. in his paper, has derived the relation between h_{21} and h_{12} with an isotropic Green's function as [12]

$$h_{21}(\bar{\sigma'}, \bar{\sigma}) = 2jkn(\bar{\sigma}) cos\theta G(\bar{\sigma}, \bar{\sigma'}), \tag{6}$$

$$h_{12}(\bar{\sigma}, \bar{\sigma'}) = 2jkn(\bar{\sigma'}) cos\theta G(\bar{\sigma'}, \bar{\sigma}). \tag{7}$$

where, $n(\bar{\sigma})$ and $n(\bar{\sigma'})$ are the refractive indices at respective source points, for all $\bar{\sigma} \in A_1$, $\bar{\sigma'} \in A_2$. θ is the angle between the z axis and the vector from $\bar{\sigma'}$ to $\bar{\sigma}$. Here, we assume z axis to be the direction of propagation of the beam and both $\bar{\sigma}$ and $\bar{\sigma'}$ lie along z axis. Hence, $\theta = 0$ and $cos\theta = 1$. The Green's function of a wave equation due to the point source is reciprocal. The proof can be found in ref [12]. The next part of the analysis will establish that the refractive indices at two different source point A_1 and A_2 embedded in an anisotropic turbulent media are different.

B. Refractive index structure function

The average refractive index value at a given place, $\bar{\sigma}$, is not a constant and varies across a wide range of length scales. The random process $n(\bar{\sigma})$ cannot therefore be regarded as a homogeneous (or spatially stationary) process. Instead of focusing on the random process $n(\bar{\sigma})$ directly, we will use the structure function, which can be defined as another random process that behaves very similar to a stationary random process with slowly varying mean and is given by,

$$D(\bar{\sigma}, \bar{\sigma'}) = \left\langle \left[n(\bar{\sigma}) - n(\bar{\sigma'}) \right]^2 \right\rangle. \tag{8}$$

Hence, $D(\bar{\sigma}, \bar{\sigma'})$ denotes the mean-square difference in the refractive index at points $\bar{\sigma}$ and $\bar{\sigma'}$. The refractive index structure constant C_n^2 is a measure of atmospheric turbulence at any given point and for an eddy of scale size l, the refractive index fluctuations are given by [5]

$$\left\langle [\delta n(l)]^2 \right\rangle = C_n^2 l^{2/3}. \tag{9}$$

Aperture A_1 is embedded in a strong turbulence region and the eddies surrounding it are small and isotropic. Hence, the Kolmogorov power spectrum model of the refractive index is correct within the inertial sub-range. However, Aperture A_2 which is generally embedded in stratosphere is surrounded by optical turbules which are anisotropic at large scales and the Kolmogorov power spectrum does not accurately capture the genuine turbulence behavior. The outer scale of turbulence in the horizontal direction can be significantly larger than that in the vertical direction, according to experimental data [6, 7]. These eddies often have a horizontal size of tens of meters or, occasionally, kilometers. The size of outer scale cells in a vertical direction is typically limited to a few meters. In other words, the air density abnormalities in the stratosphere are extended along the Earth's surface giving them their distinctive characteristics. Anisotropy is typically present above the atmospheric boundary layer, which rises to an altitude of about 2 km and it is more pronounced for big turbulence cells or eddies. Toselli, Italo [2] introduced the concept of anisotropy at different scales for modelling

atmospheric turbulence and gave the relation for the structure function similar to the one of Kolmogorov but with vertical anisotropy as:

$$D_n(R) = C_n^2.R^{2/3} = C_n^2.\left[\frac{R_{xy}^2}{\zeta^2(R_{xy})} + z^2\right]^{\frac{1}{3}} \; l_0 \ll R_{xy} \ll L_0. \tag{10}$$

where, R is the seperation between two points, $\zeta = \zeta(R_{xy})$ is a function that describes how anisotropy is distributed for each turbulence cell size R_{xy} which is the radius of the turbulence cell over the plane $z = 0$.

- According to (9), one important dimension of atmospheric turbulence is the typical maximum size of individual eddies formed in the atmosphere. The size of the turbulent eddy surrounding the source apertures A_1 and A_2 as well as the refractive index structure constant will both affect the refractive index fluctuation at those apertures.
- From the famous $H - V_{5/7}$ model [14] we know that the value of C_n^2 decreases with height as we move upwards. Also, as discussed above aperture A_1 is surrounded by small and isotropic turbulent cells whereas eddies near aperture A_2 are very large and anisotropic. This leads to the conclusion that $n(\bar{\sigma}) \neq n(\bar{\sigma'})$.
- As a result, there is an asymmetry between the upward and downward propagation of the laser beam and the impulse responses $h_{21}(\bar{\sigma'}, \bar{\sigma}) \neq h_{12}(\bar{\sigma}, \bar{\sigma'})$.
- From (8), (9), and (10) we see that turbulent cell size as well as refractive index changes between the two sites affect how the correlations in intensity fluctuations near the two apertures, A_1 and A_2, behave.

C. Optical effects due to channel asymmetry

The relationship between the beam diameter, d_B , and the inhomogeneity dimension, l , determines how air turbulence manifests itself [10]. Turbulence's main impact is the overall deflection of the beam if $d_B/l \ll 1$. The beam appears to perform a two-dimensional random walk on the receiver plane in this case. For $d_B/l \approx 1$, the inhomogeneities operate as lenses that focus or defocus all or portions of the beam, giving the beam cross-section a granular structure. Small sections of the beam individually diffract, and the beam phase fronts are severely deformed, if $d_B/l \gg 1$. Fig. 3 depicts turbulence effects for extreme cases when $d_B/l \gg 1$ and $d_B/l \ll 1$.

1) Beam effect on air-based receiver: The HAP receiver for a ground-based transmitter will be surrounded by large eddies. The laser beam will experience some refraction, which will cause the beam to stray from its original path as the beam width remains smaller than the outer scale of turbulence ($d_B/l \ll 1$). Therefore, both the scintillation and the beam tilt effects will have an impact on the optical irradiance at the receiver. Experiments have demonstrated that power fluctuations brought on by beam tilt can often be far larger than those brought on by scintillation [15]. The scintillation index for a laser beam at a given distance L can be broken down into two parts: the scintillation on axis, at the beam's centre point,

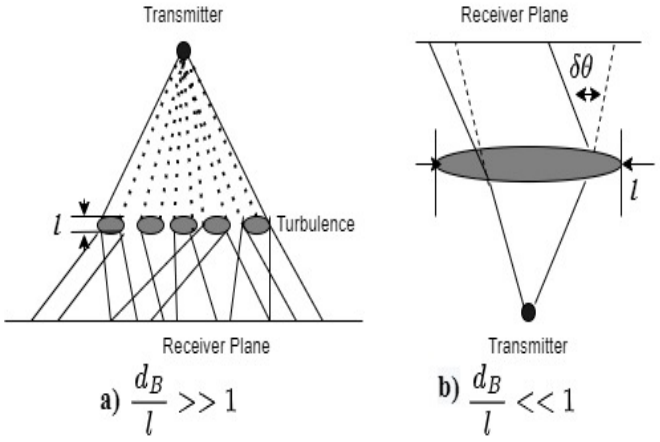

Fig. 3: Effects of atmospheric turbulence based on the relationship between beam width and turbulence dimension.

and the dependence of the scintillation on the distance to the spot's centre. The scintillation index at a receiver situated at distance L from the transmitter can be given as [15]

$$\sigma_I^2(r, L) = \sigma_I^2(0, L) + \sigma_{I,r}^2(r, L). \tag{11}$$

In optical communications, the probability distribution of the amplitude or intensity variation is crucial. Beyond the atmospheric boundary layer (1-2km) the turbulence is weak and theoretically the application of the central limit theorem leads to a normal distribution of the log-amplitude i.e. the scintillation follows a log-normal distribution. For a unit-amplitude plane wave, the probability density of intensity $p(I)$ satisfies

$$p(I) = \frac{1}{[(2\pi)^{1/2}\sigma I]} exp\left[-\frac{(\ln I + (\sigma^2/2))^2}{2\sigma^2}\right]. \tag{12}$$

In the physical model proposed by deWolf [16] the field component at the receiver that is forward scattered by the eddies on the propagation axis can be denoted by $Iexp(i\phi)$, where the phase ϕ is Gaussian distributed and the amplitude I satisfies the log normal distribution given by (12). Since, the receiver is in close proximity of the large sized eddies, there will be field due to all different off-axis components which can be denoted by $Ae^{i\theta}$. Different off-axis eddies will cause the random displacement of the spot centroid and since these contributions are all statistically independent, then by central limit theorem A appears to follow a Rayleigh distribution of probability given by

$$p(A) = \frac{2A}{< A^2 >} exp\left[-\frac{A^2}{< A^2 >}\right]. \tag{13}$$

Due to finite transverse dimensions of real laser beams, we must take into account beam tilt effect in addition to scintillation effects. Let, $\hat{U}$ denote the amplitude of the total field at the receiver which is the sum of the two components discussed earlier. The probability density for the amplitude $\hat{U}$ can be written as

$$p(\hat{U}) = \frac{2\hat{U}}{(2\pi)^{1/2}\sigma < A^2 >} \int_0^\infty \frac{1}{I} I_0 \left(\frac{2\hat{U}I}{< A^2 >} \right) .exp \left[-\frac{(\ln I + (\sigma^2/2))^2}{2\sigma^2} - \frac{\hat{U}^2 + I^2}{< A^2 >} \right] dI. \quad (14)$$

where $I_0(\cdot)$ is the zeroth-order modified Bessel function.

2) Beam effect on ground-based receiver: Eddies are isotropic and tiny near the earth's surface. The primary effects of turbulence for a ground-based receiver will be beam spreading and scintillation because the eddy size will be much less than the beam width ($d_B/l \gg 1$). Since C_n^2 (the degree of refractive index fluctuations) is highest near the earth, ground-based receivers will experience strong turbulence and hence multiple self- interference effects may be seen (Fig. 3. part (a)). For this region, the measured data show greater deviations from log-normal statistics [3]. The moderate-to-strong turbulent fading is approximately modelled by the (normalised) gamma-gamma distribution [3].

$$p(\hat{U}) = \frac{2(\alpha\beta)^{(\alpha+\beta)/2}}{\Gamma(\alpha)\Gamma(\beta)} \hat{U}^{\frac{(\alpha+\beta)}{2}-1} K_{\alpha-\beta}(2\sqrt{\alpha\beta\hat{U}}); \hat{U} > 0. \quad (15)$$

where $\hat{U}$ denotes the amplitude fading caused by turbulence. α and β are large-scale and small-scale scintillation parameters, respectively, and $K_\nu(\cdot)$ is the modified Bessel function of the second kind and order ν. As the turbulence along the path is strong, the beam splits into several patches due to the intense turbulence and there is little wander.

The traditional approach for decreasing received power variations has been to enlarge the receiving optics, often known as aperture averaging. As a result, the diameter of the ground-based receiver aperture may be increased to reduce the fluctuations in the received power. But the size of an air-based receiver cannot be very large and hence the atmospheric turbulence-induced fluctuations will naturally have a more severe impact on an air-based receiver in comparison to a ground-based receiver.

IV. Numerical Results

Phase screen simulation model is used to see the effects of the atmosphere on the propagating beam. The phase screens are generated using an anisotropic atmospheric power spectrum. The atmosphere is divided into segments of length δh_i and for each region the phase screens carry the integrated phase changes induced to the beam due to turbulence over distance δh_i. After that, the phase screen is positioned at the beginning of the propagation length, with the rest of the atmosphere's refractive index assumed to be constant. The result at the end of the entire propagation length is a beam that has been deformed mimicking the effects of the turbulent eddies in the atmosphere. Thus, this process recreates what a receiver with an intensity detector would observe. The beam is numerically represented by a grid of uniform pixels, each of which has a complex number assigned to it and the propagation is modeled

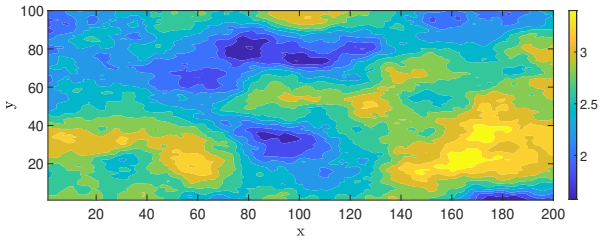

Fig. 4: Sample phase screen for $C_n^2 = 10^{-13}m^{2/3}$.

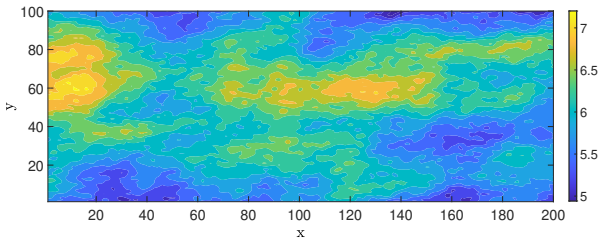

Fig. 5: Sample phase screen for $C_n^2 = 10^{-17}m^{2/3}$.

using a Fourier method. The simulations are repeated 100000 times to accurately estimate the channel parameters because the outcome of each beam propagation is random. The widely adopted $H - V_{5/7}$ model [14] was used to generate the values of refractive index structure constant varying with height to accommodate variable turbulence strengths. The empirical Coulman–Vernin profile [17] is used to model outer scale of turbulence L_0 as a function of the altitude h and the inner scale l_0 is set as $l_0 = 0.005L_0$. Fig. 4 and Fig. 5 shows two samples of the phase screens used when the structure function for the refractive index fluctuations is $C_n^2 = 10^{-13}m^{2/3}$ and $C_n^2 = 10^{-17}m^{2/3}$ respectively. Fig. 6 shows the transmitted Gaussian beam profile. The probability density function (PDF) of irradiance for forward and reverse propagation of the beam are plotted in Fig. 7 and Fig. 8. For an optical ground-based transmitter, the receiver is embedded in a weak turbulence regime and the PDF of irradiance can be seen to follow a log-normal distribution. Analytical log-normal PDF is also plotted

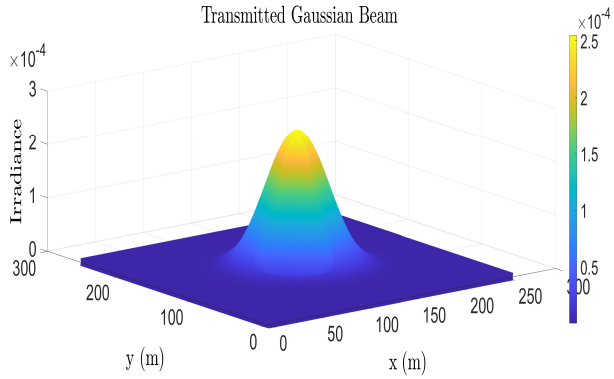

Fig. 6: Transmitted Gaussian beam.

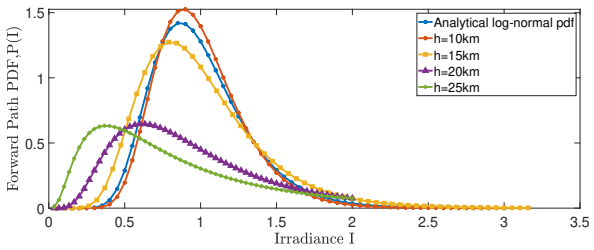

Fig. 7: Probability distribution of beam irradiance in the ground-to-HAP propagation path.

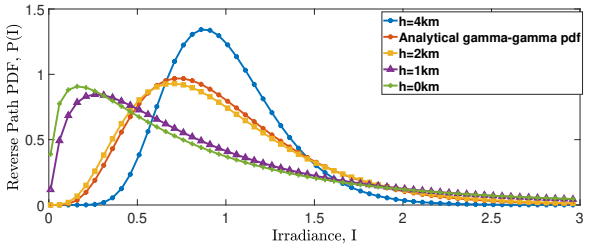

Fig. 8: Probability distribution of beam irradiance in the HAP-to-ground propagation path.

for comparison. As the height increases, the size of turbulent eddies increases and the beam tilting effect starts showing. In Fig. 7 we see that at a height of 10 km where the turbulence is weak the probability distribution of irradiance is close to log-normal. However, as the beam travels further up, it encounters large eddies and the beam wandering effect begins to manifest. As a result, the PDF of irradiance start deviating from the log-normal distribution and significant beam wandering effect can be seen at height 20 km and above.

For an air-based transmitter and a ground receiver the turbulence effects are strong and gamma-gamma PDF distribution is obtained. In Fig. 8 we see that for a beam traveling from HAP transmitter up to a height of 4km, the beam has travelled in weak turbulence region so far and the PDF follows a log-normal distribution. But, as height starts decreasing and the beam enters the atmospheric boundary layer where the turbulence strength is strong, the distribution of irradiance changes to gamma-gamma distribution model. We have plotted the probability distribution of irradiance of the beam at various heights as it is travelling in the atmospheric boundary layer before finally approaching the ground-based optical receiver.

V. Conclusion

In this paper, we investigated the influence of different atmospheric turbulence cells on the propagation of the laser beam. Our study demonstrated that the typical maximum size and shape of individual eddies adjacent to the optical receiver have a substantial impact on the variability in received optical power. Through phase screen simulations, we were able to verify that the asymmetry in the forward and backward routes of the bi-directional laser links would lead to different Gaussian beam power distributions at the receiver. The findings from this study on the asymmetrical features of bi-directional laser links will enable high-performance ground-to-HAP communications in real FSO channels.

VI. Acknowledgement

This work was supported in part by the Science and Engineering Board, Department of Science and Technology (DST), Government of India, under Grant CRG/2019/002293; in part by the Indian National Academy of Engineering (INAE) through the Abdul Kalam Technology Innovation National Fellowship; One of authors (S. Dharmaraja) would like to thank DST, India for providing the financial support through research project no. 64800 .

References

[1] M. Q. Vu, N. T. Nguyen, H. T. Pham, and N. T. Dang, "All-optical two-way relaying free-space optical communications for hap-based broadband backhaul networks," *Optics Communications*, vol. 410, pp. 277–286, 2018.

[2] I. Toselli, "Introducing the concept of anisotropy at different scales for modeling optical turbulence," *J. Opt. Soc. Am. A*, vol. 31, no. 8, pp. 1868–1875, Aug 2014.

[3] L. C. Andrews and R. L. Phillips, *Laser beam propagation through Random Media*. SPIE Press, 2005.

[4] F. Wang, W. Du, Q. Yuan, D. Liu, and S. Feng, "Wander of a gaussian-beam wave propagating through kolmogorov and non-kolmogorov turbulence along laser-satellite communication uplink," *Atmosphere*, vol. 13, no. 2, 2022.

[5] S. S. R. Murty, "Laser beam propagation in atmospheric turbulence," *Indian Academy of Sciences Proceedings: Section C Engineering Sciences*, vol. 2, pp. 179–195, May 1979.

[6] M. Yao, I. Toselli, and O. Korotkova, "Propagation of electromagnetic stochastic beams in anisotropic turbulence," *Opt. Express*, vol. 22, no. 26, pp. 31 608–31 619, Dec 2014.

[7] A. Zilberman, E. Golbraikh, and N. S. Kopeika, "Propagation of electromagnetic waves in kolmogorov and non-kolmogorov atmospheric turbulence: three-layer altitude model," *Appl. Opt.*, vol. 47, no. 34, pp. 6385–6391, Dec 2008.

[8] D. T. Kyrazis, J. B. Wissler, D. D. B. Keating, A. J. Preble, and K. P. Bishop, "Measurement of optical turbulence in the upper troposphere and lower stratosphere," in *Laser Beam Propagation and Control*, vol. 2120, International Society for Optics and Photonics. SPIE, 1994, pp. 43 – 55.

[9] S. Halsig, T. Artz, A. Iddink, and A. Nothnagel, "Using an atmospheric turbulence model for the stochastic model of geodetic vlbi data analysis," *Earth, Planets and Space*, vol. 68, pp. 1–14, 2016.

[10] W. K. Pratt, *Laser communication systems [by] William K. Pratt*. Wiley New York, 1969.

[11] W. Gappmair, "Further results on the capacity of free-space optical channels in turbulent atmosphere," *IET Communications*, vol. 5, no. 9, pp. 1262–1267, 2011.

[12] J. H. Shapiro, "Reciprocity of the turbulent atmosphere*," *J. Opt. Soc. Am.*, vol. 61, no. 4, pp. 492–495, Apr 1971.

[13] A. Saleh, "9.4 - an investigation of laser wave depolarization due to atmospheric transmission," *IEEE Journal of Quantum Electronics*, vol. 3, no. 11, pp. 540–543, 1967.

[14] R. E. Hufnagel and N. R. Stanley, "Modulation transfer function associated with image transmission through turbulent media," *J. Opt. Soc. Am.*, vol. 54, no. 1, pp. 52–61, Jan 1964.

[15] F. Dios, J. A. Rubio, A. Rodríguez, and A. Comerón, "Scintillation and beam-wander analysis in an optical ground station-satellite uplink," *Appl. Opt.*, vol. 43, no. 19, pp. 3866–3873, Jul 2004.

[16] D. De Wolf, "Waves in turbulent air: A phenomenological model," *Proceedings of the IEEE*, vol. 62, no. 11, pp. 1523–1529, 1974.

[17] C. E. Coulman, J. Vernin, Y. Coqueugniot, and J. L. Caccia, "Outer scale of turbulence appropriate to modeling refractive-index structure profiles," *Appl. Opt.*, vol. 27, no. 1, pp. 155–160, Jan 1988.